

Criticality Enhanced Quantum Sensing via Continuous Measurement

Theodoros Ilias,^{1,*} Dayou Yang,^{1,*} Susana F. Huelga,¹ and Martin B. Plenio¹

¹*Institut für Theoretische Physik and IQST, Universität Ulm,
Albert-Einstein-Allee 11, D-89069 Ulm, Germany*

(Dated: May 28, 2022)

Present protocols of criticality enhanced sensing with open quantum sensors assume direct measurement of the sensor and omit the radiation quanta emitted to the environment, thereby omitting potentially valuable information. Here we propose a protocol for criticality enhanced sensing via continuous observation of the emitted radiation quanta. Under general assumptions, we establish a scaling theory for the global quantum Fisher information of the joint system and environment state at a dissipative critical point. We demonstrate that it obeys universal scaling laws featuring transient and long-time behavior governed by the underlying critical exponents. Importantly, such scaling laws exceed the standard quantum limit and can in principle saturate the Heisenberg limit. To harness such advantageous scaling, we propose a practical sensing scheme based on continuous detection of the emitted quanta. In such a scheme a single interrogation corresponds to a (stochastic) quantum trajectory of the open system evolving under the non-unitary dynamics dependent on the parameter to be sensed and the back-action of the continuous measurement. Remarkably, we demonstrate that the associated precision scaling significantly exceeds that based on direct measurement of the critical steady state, thereby establishing the metrological value of detection of the emitted quanta at dissipative criticality. We illustrate our protocol via counting the photons emitted by the open Rabi model, a paradigmatic model for the study of dissipative phase transition with finite components. Our protocol is applicable to diverse open quantum sensors permitting continuous readout, and may find applications at the frontier of quantum sensing such as human-machine interface, magnetic diagnosis of heart disease and zero-field nuclear magnetic resonance.

I. INTRODUCTION

A most ambitious vista of quantum sensing is to enhance the sensor precision from the standard quantum limit (SQL) [1–3] of independent, uncorrelated measurements towards the Heisenberg limit (HL) [4, 5], the ultimate precision allowed by quantum mechanics. Given a fixed number N of the sensor components and a total time t of the sensing interrogation, the SQL represents a (classical) scaling of the estimation error as $\sim 1/\sqrt{Nt}$, whereas the HL features a quantum-enhanced scaling $\sim 1/Nt$ [6]. Such enhancement, on the one hand, can in principle be achieved by preparing individual sensor components in entangled quantum states, e.g., the Greenberger–Horne–Zeilinger (GHZ) state [7] and spin-squeezed states [6, 8]. Nevertheless, such states are technically challenging to scale up and are fragile when exposed to noise [9], and is thus far restricted to a small number of components, see recent advances [10–16]. On the other hand, alternative strategies without direct use of entangled states open up intriguing and promising routes towards quantum-enhanced sensing with affordable technological demand, see Ref. [17] for an overview.

A recent highlight among these is criticality enhanced sensing [18–24]. The key ingredient there is the universally divergent susceptibility of the ground state to small variation of parameters of Hamiltonians at quantum critical points (CPs). Such divergence translates directly into

a divergent Quantum Fisher information (QFI). Protocols of criticality enhanced sensing typically adopt one of the following two approaches. The first approach [19, 24] is based on the time evolution of the ground state following a quench of the Hamiltonian parameters across the CP, i.e., exploiting the dynamic susceptibility. The precision is quantified by the QFI of the time-evolved state, which obeys a sub-Heisenberg scaling $\sim t^2 N^\alpha$ with $\alpha \leq 2$ determined by the critical exponents of the underlying CP. The second approach [18, 23] exploits the static susceptibility of the ground state, by adiabatically switching the Hamiltonian parameters across the CP. The precision is quantified by the QFI of the ground state, which may obey an apparent super-Heisenberg scaling with respect to N . This, however, comes at the price of a divergent interrogation time to maintain adiabaticity close to the CP [20]. Taking into account such time, the ground-state QFI obeys the same scaling $\sim t^2 N^\alpha$ as in the quench approach [20]. Therefore, the two approaches are equivalent and both provide a promising avenue towards the HL based on engineering short-range interacting many-body systems close to quantum criticality. Experimentally, such a capability has been demonstrated in various quantum-optical setups well isolated from the environment [25–28].

Open quantum systems represent another interesting candidate for criticality enhanced sensing. These systems support dissipative criticality [32–37], defined via gap closing in the lowest (real) spectrum of the Liouville super-operator for the reduced density matrix of the system. At a dissipative CP, the thermodynamic properties of the steady density matrix manifest divergent scal-

* T. I. and D. Y. contributed equally to this work.

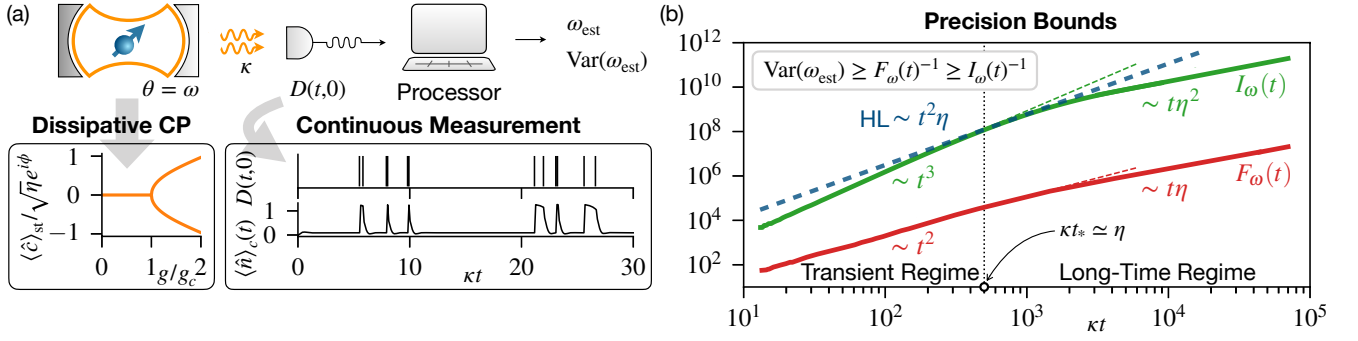


FIG. 1. (a) The open Rabi model as a model system demonstrating criticality enhanced sensing via continuous measurement. We consider the sensing of the cavity mode frequency ω as an illustration. The cavity leaks photons at a rate κ , counted continuously by a photon detector. The model parameters are tuned to a dissipative CP g_c , where its steady state undergoes a continuous phase transition (see text). Here η is the effective system size, $\phi = \arctan(2\kappa/\omega)$. A sensing interrogation corresponds to a quantum trajectory consisting of the continuously detected signal $D(t,0)$ and the associated conditional evolution of the open system, as exemplified by the cavity mode occupation $\langle \hat{n} \rangle_c(t)$. Processing $D(t,0)$ (e.g., via Bayesian inference [29–31]) provides an estimator ω_{est} with an imprecision (variance) $\text{Var}(\omega_{\text{est}})$. (b) Scaling of the precision bounds at dissipative criticality, including the global QFI of the joint system-environment $I_\omega(t)$, and the FI $F_\omega(t)$ of the detected signal. Both quantities manifest algebraic scaling with respect to t and η , and for illustration we show the numerical results for $\eta = 500$. With respect to the interrogation time t , the precision bounds obeys (super-)Heisenberg scaling in the transient regime, $t \lesssim t_* \simeq \eta/\kappa$, whereas linear scaling in the long-time regime, $t \gg t_*$. The scaling should be contrasted with the HL $\sim t^2 \eta$ (thick dashed blue) and the SQL $\sim t \sqrt{\eta}$ (not shown). The scaling exponents of the global QFI can be related to the critical exponents $z = 1$, $\Delta_{\hat{n}} = -1/2$ and the spatial dimension $d = 0$ via the general formulas (13) and (14).

ing behavior, bearing similarities to the behavior of the ground state at a quantum CP.

State-of-the-art protocols [21–23] for critical open sensors quantify the sensor precision limit via the QFI of the reduced density matrix of the system. This, however, only represents the optimal precision achieved by direct measurement of the system alone. In stark contrast to closed systems, open dissipative systems continuously exchange radiation quanta with their environments, which carry information about the system and therefore, about the parameter to be sensed. Such radiation quanta may be detected continuously in time via mature experimental techniques in quantum optics, e.g., photon counting and homodyne measurement [38–41], accomplishing indirect monitoring of the system via measurement of the environment. Such a unique opportunity makes open sensors a natural platform for implementing continuous-measurement-based sensing schemes [29–31, 42–44] and, from a theoretical point of view, requires the use of the global QFI of the joint system-environment state $|\Psi(t)\rangle$

$$I_\theta(t) = 4[\langle \partial_\theta \Psi(t) | \partial_\theta \Psi(t) \rangle - |\langle \Psi(t) | \partial_\theta \Psi(t) \rangle|^2] \quad (1)$$

as the ultimate precision bound, which can in principle be achieved by the most general measurement of the joint system-environment (implementing such measurement in practice, however, may be challenging). This has been emphasized in sensing with non-interacting open system [29–31, 42] and systems manifesting first-order dynamic phase transitions [45], as well as in scenarios of noisy quantum sensing with observed environments [46, 47].

In contrast to the existing studies [29–31, 42, 45–47],

here we are interested in open quantum many-body sensors at (continuous) dissipative CPs. Two questions emerge naturally in this context. (i) Does the global QFI (1) manifest criticality-enhanced universal scaling at a dissipative CP? (ii) If so, can we access such enhanced precision scaling via realistic measurement schemes of the emitted radiation quanta? In this manuscript, we provide positive answers to both questions. We show that the global QFI (1) for a generic Markovian open sensor obeys universal scaling laws at dissipative criticality, which are governed by the universal critical exponents of the underlying CP. Such scaling exceeds the SQL, and can in principle saturate the HL. Moreover, as a practical scheme to access the criticality-enhanced precision, we analyze a continuous-measurement-based sensing protocol applicable to the sensing of arbitrary parameters at generic dissipative CPs.

Our key findings are illustrated in Fig. 1 at the example of the open Rabi model (see Refs. [48] and below), a paradigmatic model for the study of dissipative phase transition with finite components. Panel 1 (a) presents a schematic of our sensing protocol. We assume the open system is tuned to a dissipative CP. The quantity we wish to sense, θ , is encoded as a parameter in the system Hamiltonian. A single sensing interrogation consists of initializing the system at $t_0 = 0$ in the same (arbitrary) state and subsequent detection and evolution spanning $[0, t)$. We emphasize such evolution is subjected to measurement back-action randomly driving the system away from the steady state, in stark contrast with the steady-state based scenario [21, 23]. As such, our scheme has the natural advantage that it does not require steady-state

preparation which typically suffers critical slowing down. Detection of the radiation quanta continuously in time provides us with measurement signals $D(t, 0)$ dependent on the system dynamics, that is, on θ . This allows us to construct an estimator θ_{est} . The associated precision can be quantified by the Fisher information (FI) of the detected signal

$$F_\theta(t) = \sum_{D(t,0)} P[D(t,0)] \{ \partial_\theta \ln P[D(t,0)] \}^2, \quad (2)$$

where $P[D(t,0)]$ is the probability of the continuously detected signal $D(t,0)$. According to the Cramér-Rao inequality [49], the FI sets a lower bound to the variance of any (unbiased) estimator of θ , i.e., $\text{Var}(\theta_{\text{est}}) \geq 1/F_\theta(t)$.

The universal scaling of the precision bounds is exemplified in Panel 1(b) by the sensing of the cavity mode frequency, $\theta = \omega$. We find that the time dependence of both the global QFI and the FI can be divided into two regimes, the transient regime and the long-time regime, separated by a characteristic time scale $t_* \simeq \eta/\kappa$, with η the effective size of the system and κ the cavity damping rate. In the transient regime, $t \lesssim t_*$, the global QFI obeys a super-Heisenberg scaling with respect to time $I_\omega(t) \sim t^3$ whereas the FI obeys the Heisenberg scaling $F_\omega(t) \sim t^2$. In the long-time regime, $t \gg t_*$, both quantities grow linearly in time, and depend algebraically on the system size η , $I_\omega(t) \sim \eta^2 t$ and $F_\omega(t) \sim \eta t$. The scaling exponents of the global QFI can be expressed analytically in terms of the critical exponents of the underlying CP.

The rest of the manuscript is organized as follows. In Sec. II, we discuss the universal scaling behavior of the global QFI (1) at a generic dissipative critical point. Afterwards, we analyze in Sec. III a continuous-measurement based sensing protocol for accessing the criticality-enhanced precision, illustrated at the example of the open Rabi model. We conclude in Sec. IV with a summary of our results and an outlook.

II. UNIVERSAL SCALING OF THE GLOBAL QUANTUM FISHER INFORMATION

Let us start our discussion by analyzing the precision limit of a generic open quantum sensor at dissipative criticality. Consider the sensor as an open many-particle system with spatial extension L defined on a d -dimensional lattice, consisting of $N = L^d$ interacting particles as individual sensor components. We assume the open system is coupled to a Markovian environment at zero temperature, and the reduced density matrix of the unobserved system evolves according to a Lindblad master equation (LME) [50–53] (we set $\hbar = 1$ hereafter)

$$\dot{\rho} = \mathcal{L}\rho \equiv -i[\hat{H}(\theta), \rho] + \sum_\ell \left(\hat{J}_\ell \rho \hat{J}_\ell^\dagger - \frac{1}{2} \{ \hat{J}_\ell^\dagger \hat{J}_\ell, \rho \} \right). \quad (3)$$

We consider the sensing of a single quantity θ which, without the loss of generality, is assumed to be encoded as

a parameter of the many-body Hamiltonian $\hat{H}(\theta)$. $\{\hat{J}_\ell\}$ represents a set of (single- or many-body) jump operators resulting from system-environment coupling, with ℓ the set index. To be specific, we focus on the experimentally common situation where θ is encoded in single-body terms,

$$\hat{H}(\theta) = \sum_{i=1}^N \hat{h}_i(\theta) + \sum_{i<j}^N \hat{h}_{ij} + \dots, \quad (4)$$

i.e., we assume all n -body ($n \geq 2$) terms describing inter-particle interactions are θ -independent.

The sensor precision is upper-bounded by the global QFI (1), which may be achieved by the most general measurement performed on the joint system-environment state $|\Psi(t)\rangle$. Interestingly enough, assuming the validity of the quantum regression theorem, such a global QFI can be expressed solely in terms of the system auto-correlators [42],

$$I_\theta(t) = 2 \int_0^t d\tau \int_0^\tau d\tau' \langle \{ \delta \hat{O}(\tau'), \delta \hat{O}(\tau) \} \rangle. \quad (5)$$

Here, $\hat{O} := \partial_\theta \hat{H}(\theta)$ is the Hermitian operator which encodes θ , the angle bracket $\langle \dots \rangle := \text{tr}[\dots \rho(0)]$ denotes an expectation with respect to the initial (pure) system density matrix $\rho(0) = |\psi(0)\rangle\langle\psi(0)|$, and $\delta \hat{O}(t) := \hat{O}(t) - \langle \hat{O}(t) \rangle$. Under our assumption Eq. (4), $\hat{O} = \sum_{i=1}^N \hat{o}_i$ is an extensive single-body operator, with $\hat{o}_i := \partial_\theta \hat{h}_i(\theta)$ the local operator of the i -th particle. The global QFI (5) can therefore be expressed as

$$I_\theta(t, L) = 8L^d \int_0^t d\tau \int_0^{t-\tau} ds S(\tau, s, L), \quad (6)$$

$$S(\tau, s, L) = \frac{1}{L^d} \sum_{i,j=1}^N \Re[\langle \delta \hat{o}_i(\tau + s) \delta \hat{o}_j(\tau) \rangle], \quad (7)$$

in which \Re denotes the real part, and we have indicated explicitly the dependence of the global QFI on the system size L . Equations (6) and (7) provide us with a useful connection between the global QFI and the auto-correlators of the open quantum sensor. In particular, as we show below, they lead to explicit quantitative predictions at continuous dissipative CPs, where the universal scaling laws of the auto-correlators translate directly into the scaling of the global QFI.

A. Criticality and universal scaling

Let us assume that the LME (3) supports a continuous dissipative CP in its steady state ρ_{st} , i.e., the solution of the stationary LME $\mathcal{L}\rho_{\text{st}} = 0$. We assume h is a parameter of the LME (3) that drives the system across the phase transition (h can be independent of θ), and the CP is located at $h_c = 0$. Close to the CP, the static and dynamic properties associated with ρ_{st} obey universal scaling laws

governed by a small number of critical exponents. In the following we show that the global QFI (6) manifests such universal scaling behavior.

To begin with, we introduce

$$S_{\text{st}}(s, L) = \frac{1}{L^d} \sum_{i,j=1}^N \Re[\langle \delta \hat{o}_i(s) \delta \hat{o}_j(0) \rangle_{\text{st}}], \quad (8)$$

with $\langle \cdots \rangle_{\text{st}} := \text{tr}(\rho_{\text{st}} \cdots)$ an expectation value with respect to the steady state. Note that $S_{\text{st}}(0, L)$ is the static structure factor of the steady state at zero momentum. Assuming translational invariance, and taking the thermodynamic limit $L \rightarrow \infty$, $S_{\text{st}}(0, L)$ obeys the well-known scaling behavior (see, e.g., Ref. [54]) $S_{\text{st}}(0, L) \sim \xi^{d-2\Delta_\delta}$, provided $d - 2\Delta_\delta > 0$, where Δ_δ is the scaling dimension of the operator \hat{o}_i , defined via $\langle \delta \hat{o}_i(0) \delta \hat{o}_{i+r}(0) \rangle_{\text{st}} \sim r^{-2\Delta_\delta}$ at the CP $h_c = 0$. ξ is the correlation length of the system, which diverges according to $\xi \sim h^{-\nu}$ close to the CP, with ν the correlation-length critical exponent. In the opposite case of $d - 2\Delta_\delta \leq 0$, $S_{\text{st}}(0, L) \sim \text{const.}$ dependent on the short-distance (ultra-violet) cut-off, i.e., it is not universal. For correlations of non-equal time $s \neq 0$ and of finite system-size L , the above scaling behavior can be generalized to a dynamic scaling form [55, 56]

$$S_{\text{st}}(s, L) = \Lambda^{d-2\Delta_\delta} \phi_{\text{st}}(\Lambda^{1/\nu} h, \Lambda^z s^{-1}, \Lambda L^{-1}), \quad (9)$$

in which Λ is a cut-off length scale determined by the relative strength of the two perturbations to the CP, h and L^{-1} , ϕ_{st} is a universal function and z is the dynamic critical exponent. If h is sufficiently small, $h \ll L^{-1/\nu}$, the inverse system size L^{-1} is the most relevant perturbation to the CP, i.e., the finite-size effect most severely drives the system away from criticality. Correspondingly, $\Lambda \simeq L$. In the opposite limit $h \gg L^{-1/\nu}$, h is the dominant perturbation to the CP. Correspondingly, $\Lambda \simeq \xi \sim h^{-\nu}$.

We now analyze the scaling behavior of $S(\tau, s, L)$, cf. Eq. (7), via analogy with Eq. (9). Note that the quantum regression theorem prescribes $\langle \delta \hat{o}_i(\tau + s) \delta \hat{o}_j(\tau) \rangle = \text{tr}[\delta \hat{o}_i e^{\mathcal{L}s} \delta \hat{o}_j e^{\mathcal{L}\tau} \rho(0)]$, and therefore, the auto-correlator $S(\tau, s, L) \rightarrow S_{\text{st}}(s, L)$ in the limit $\tau \rightarrow \infty$. Consequently, the parameter τ^{-1} can be regarded as another perturbation to the CP that controls the scaling behavior of $S(\tau, s, L)$. Assuming τ^{-1} is a relevant perturbation (in the renormalization group sense), and $d - 2\Delta_\delta > 0$, we write down a dynamic scaling ansatz

$$S(\tau, s, L) = \Lambda^{d-2\Delta_\delta} \phi(\Lambda^{1/\nu} h, \Lambda^z \tau^{-1}, \Lambda^z s^{-1}, \Lambda L^{-1}), \quad (10)$$

where the cut-off length scale Λ is determined by the relative strength of the relevant perturbations h , τ^{-1} and L^{-1} . Equation (10) provides us with a simple yet powerful scaling form for auto-correlators close to dissipative criticality, which leads directly to the scaling laws of the global QFI via Eq. (6), as shown in the next section.

We emphasize that at this stage Eq. (10) should be viewed as a tentative ansatz, the validity of which should be checked, e.g., via numerical finite-size scaling once the

model is specified. In appendix A, we provide such numerical validation for the model system (the open Rabi model, to be introduced in Sec. III A) considered in the present work.

B. Scaling laws of the global quantum Fisher information

We now study the scaling laws of the global QFI (6), based on the scaling ansatz (10). First, we note that Eq. (10) allows us to identify different regimes where the cutoff length scale Λ is set by different perturbations to the CP among h , L^{-1} and τ^{-1} , and correspondingly $S(\tau, s, L)$ obeys different scaling forms. For criticality enhanced sensing, we consider $h = 0$, i.e., the system parameter is tuned at the CP. Consequently, $S(\tau, s, L)$ picks up the following scaling forms

$$S(\tau, s, L) = \tau^{(d-2\Delta_\delta)/z} \phi_\tau(\tau s^{-1}, \tau L^{-z}), \quad \tau \lesssim L^z, \quad (11)$$

$$= L^{d-2\Delta_\delta} \phi_L(L^z \tau^{-1}, L^z s^{-1}), \quad \tau \gg L^z. \quad (12)$$

in which ϕ_τ and ϕ_L are universal scaling functions inherited from ϕ in Eq. (10).

Plugging these scaling forms into Eq. (6), we see immediately that the global QFI manifests two distinct scaling behavior dependent on the total interrogation time t compared to the system size L . (i) $t \lesssim L^z$, which is referred to as the transient regime hereafter, where the integrand $S(\tau, s, L)$ obeys the scaling form (11). (ii) $t \geq L^z$, which is referred to as the long-time regime hereafter, where $S(\tau, s, L)$ picks the form (12) in most of the integration interval in Eq. (6). Completing the integration in Eq. (6) in the two regimes we find

$$I_\theta(t, L) \sim t^{(d-2\Delta_\delta)/z+2} L^d, \quad t \lesssim L^z, \quad (13)$$

$$\sim t L^{2d-2\Delta_\delta+z}, \quad t \gg L^z. \quad (14)$$

In arriving at Eq. (14), we have made the approximation $\int_0^{t-\tau} ds \simeq \int_0^\infty ds$, justified by the fact that $\phi_L(L^z \tau^{-1}, L^z s^{-1}) \rightarrow 0$ sufficiently fast at large s/L^z as a result of the finite correlation time in a finite-size system.

Equations (13) and (14) serve as the central formulas of this section, which provide us with the scaling laws of the global QFI (1) of a generic (Markovian) open quantum sensor at dissipative criticality. Such scaling depends on the spatial dimension d , the dynamic critical exponent z and the scaling dimension of the local operator \hat{o}_i that encodes the unknown parameter.

C. Super-Heisenberg scaling and consistency with the Heisenberg limit

Let us discuss a few peculiar features of the scaling laws in Eqs. (13) and (14), cf. Fig. 2. First, we note that they surpass the SQL, and are improved further by coupling θ to operators with a small scaling dimension Δ_δ .

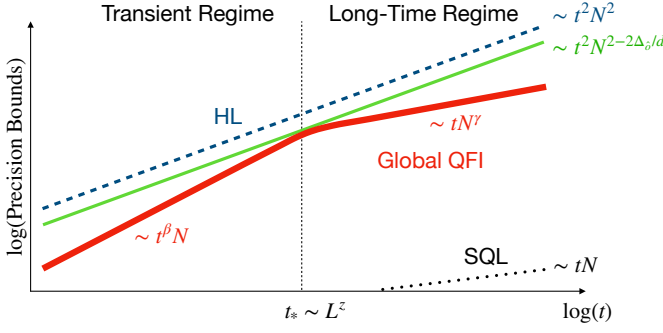


FIG. 2. Illustration of the universal scaling laws of the global QFI at a generic dissipative CP, Eqs. (13) and (14), with respect to the interrogation time t and the particle number $N \equiv L^d$, assuming $d \geq 1$. The global QFI (thick red solid), its tight bound Eq. (15) (light green solid), are contrasted with the HL (dark blue dashed) and the SQL (black dotted). The characteristic time scale $t_* \sim L^z$ separates the transient regime and the long-time regime, where the global QFI obeys different scaling laws. The scaling exponents are determined by the spatial dimension d , the dynamic critical exponent z and the scaling dimension Δ_δ of the local operator \hat{o}_i that encodes the unknown parameter, via $\beta = 2 + (d - 2\Delta_\delta)/z$ and $\gamma = 2 + (z - 2\Delta_\delta)/d$.

Such a condition is met typically by relevant operators (in the renormalization group sense) of low-dimensional CPs [20].

Second, we compare the scaling laws in Eqs. (13) and (14) to the HL widely discussed in the context of interferometric sensing [4, 5]. We focus on the case that \hat{o}_i is a single-body operator, and we temporarily assume $d \geq 1$. Therefore, the HL adopts the familiar expression $\text{HL} \sim t^2 N^2 \equiv t^2 L^{2d}$. We comment on the special case $d = 0$ at the end of this section.

One interesting aspect is the apparent super-Heisenberg scaling with respect to the interrogation time t or the particle number N in different regimes. In the transient regime $t \lesssim L^z$, the global QFI [cf. Eq. (13)] manifests super-Heisenberg scaling with respect to t [note that we assume $d - 2\Delta_\delta > 0$ for the validity of Eqs. (13) and (14)] whereas linear scaling with respect to N . In the long-time regime $t \gg L^z$, the global QFI [cf. Eq. (14)] manifests linear scaling in t and super-Heisenberg scaling in N , provided by the condition $z - 2\Delta_\delta > 0$, which can be fulfilled by encoding θ in operators with small scaling dimensions.

Despite such apparent super-Heisenberg scaling, the global QFI is indeed upper-bounded by the HL. To see this, let us introduce the precision scaling

$$I_\theta^*(t, L) \sim t^2 L^{2d-2\Delta_\delta}. \quad (15)$$

We note that for continuous CPs defined in spatial dimensions $d \geq 1$, the operator scaling dimensions are positive, $\Delta_\delta \geq 0$. Therefore, the scaling (15) is sub-Heisenberg. Dividing both sides of Eqs. (13) and (14) by

$$I_\theta^*(t, L),$$

$$I_\theta(t, L)/I_\theta^*(t, L) \sim (tL^{-z})^{(d-2\Delta_\delta)/z}, \quad t \lesssim L^z, \quad (16)$$

$$\sim L^z t^{-1}, \quad t \gg L^z. \quad (17)$$

Therefore, $I_\theta(t, L) \lesssim I_\theta^*(t, L)$ in both the transient and the long-time regime. Only at the sweet spot $t_* \simeq L^z$, $I_\theta(t_*, L)$ saturate $I_\theta^*(t, L)$. This confirms that the global QFI is Heisenberg limited in $d \geq 1$.

In $d = 0$, the critical open system does not possess a rigorous spatial extension L . Consequently, the HL cannot be expressed as $t^2 L^{2d}$, and should be analyzed in terms of the actual resources involved in the sensing protocol. This is illustrated in the next section via the open Rabi model, for which we show the associated global QFI actually saturates the HL [cf., Fig. 1(b) and Sec. III B].

III. CRITICALITY ENHANCED PRECISION VIA CONTINUOUS MEASUREMENT

The universal scaling of the global QFI opens up an avenue towards enhanced precision scaling harnessing dissipative criticality. Saturating the global QFI, however, requires a most general measurement of the joint system-environment, which may be practically challenging. Do practical measurement schemes provide access to the criticality-enhanced scaling (which, in general, is lower than the scaling of the global QFI)? In this section we provide a positive answer to this question, by analyzing a readily implementable sensing protocol based on continuous measurement of the radiation quanta emitted by the open sensor. While our protocol is generally applicable to critical open systems in diverse setups that permit optical readout, to be specific in the following we illustrate it via the open Rabi model [48], a light-matter interacting model featuring a continuous dissipative CP in zero spatial dimension. Besides its conceptual simplicity, its finite-component nature facilitates numerical simulation, making it possible to extract the scaling of the (classical) Fisher information as the precision bound of our sensing scheme. As such, it allows for direct comparison between the precision scaling of our protocol and that of a recent study [23] based on direct, instantaneous measurement of the critical steady state of the open Rabi model, therefore demonstrating the advantages of our scheme.

A. Model system: the open Rabi model

Let us consider a cavity mode coupled to a qubit [cf. Fig. 1(a)] as described by the quantum Rabi Hamiltonian

$$\hat{H} = \omega \hat{c}^\dagger \hat{c} + \frac{\Omega}{2} \hat{\sigma}_z - \lambda (\hat{c} + \hat{c}^\dagger) \hat{\sigma}_x. \quad (18)$$

Here, $\hat{c}(\hat{c}^\dagger)$ denotes the annihilation (creation) operator of the cavity mode, $\hat{\sigma}_{z,x}$ are the Pauli matrices of the

qubit, ω is the cavity mode frequency, Ω is the qubit transition frequency and λ is the coupling strength. The cavity leaks photons to the external electromagnetic environment at a rate κ . Without monitoring the environment, the dynamics of the open cavity-qubit system can be described by a standard LME

$$\dot{\rho} = -i[\hat{H}, \rho] + \kappa \left(\hat{c}\rho\hat{c}^\dagger - \frac{1}{2}\{\hat{c}^\dagger\hat{c}, \rho\} \right). \quad (19)$$

Equation (19) conserves a \mathbb{Z}_2 parity symmetry $\hat{c} \rightarrow -\hat{c}$, $\hat{\sigma}_x \rightarrow -\hat{\sigma}_x$. Remarkably, in the soft-mode limit $\omega/\Omega \rightarrow 0$, the steady state of Eq. (19) can spontaneously break such a symmetry, resulting in a continuous dissipative phase transition [48].

Being zero-dimensional, the model (19) does not possess a rigorously defined system-size. Nevertheless, following [57] and [48], we can introduce the frequency ratio $\eta = \Omega/\omega$ as the ‘effective size’ of the model, with $\eta \rightarrow \infty$ corresponding to the thermodynamic limit [48]. We further introduce a dimensionless coupling constant $g = 2\lambda/\sqrt{\Omega\omega}$. In the limit $\eta \rightarrow \infty$, the system undergoes a continuous phase transition at a critical point $g_c = \sqrt{1 + (2\kappa/\omega)^2}$ [48], cf. Fig. 1(a). At $g < g_c$, the system is in the normal phase, characterized by the order parameter $\langle \hat{c} \rangle_{\text{st}} = 0$, whereas at $g > g_c$, the system enters the superradiant phase, characterized by $\langle \hat{c} \rangle_{\text{st}} \neq 0$. Finite η plays the role of a finite-size cutoff, which renders the phase transition to a smooth crossover.

The critical properties of the CP has been extracted numerically via finite-size (i.e., finite- η) scaling of various thermodynamic quantities [48], which provides $z = 1$ as the dynamic and $\nu = 2$ as the correlation length critical exponent. As such, the open Rabi model lies in the same universality class as the open Dicke model [58, 59]. At the CP $g = g_c$, the mean occupation of the cavity mode diverges according to $\langle \hat{n} \rangle_{\text{st}} \sim \eta^{1/2}$, in which $\hat{n} := \hat{c}^\dagger \hat{c}$. Therefore, the scaling dimension of \hat{n} is $\Delta_{\hat{n}} = -1/2$, which satisfies the condition $d - 2\Delta_{\hat{n}} > 0$ (cf. Sec. II B). As such, the sensing of the cavity mode frequency ω serves as a ideal demonstration of criticality enhanced sensing, which we analyze in detail below.

B. Scaling laws of the global quantum Fisher information

In Fig. 3 we show the numerical finite-size scaling of the global QFI for the sensing of ω , for different system sizes η in both the transient regime $\kappa t \lesssim \eta^z$ [Fig. 3(a)] and in the long-time regime $\kappa t \gg \eta^z$ [Fig. 3(b)], assuming the model is tuned at the CP $g = g_c$. The perfect data collapse indicates the following scaling behavior of the global QFI

$$I_\omega(t, \eta) = (\kappa t)^3 f_I(\kappa t/\eta), \quad \kappa t \lesssim \eta, \quad (20)$$

$$I_\omega(t, \eta) = \text{const.} \times \kappa t \eta^2, \quad \kappa t \gg \eta, \quad (21)$$

in which $f_I(\kappa t/\eta)$ is a universal function reflecting the finite-size correction. This validates the predictions of

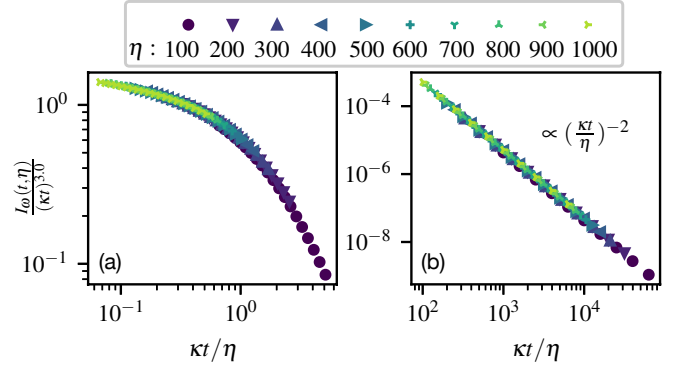


FIG. 3. Finite-size scaling of the global QFI of the critical open Rabi model plus the environment, in both (a) the transient regime $\kappa t \lesssim \eta$ and (b) the long-time regime $\kappa t \gg \eta$. The open system is at a dissipative critical point $g = g_c$, and η is its effective size (see text).

the general formulas (13) and (14) when the relevant exponents $d = 0$, $z = 1$ and $\Delta_{\hat{n}} = -1/2$ are plugged in.

The scaling laws (20) and (21) are Heisenberg-limited. As a zero-dimensional model, the HL of the open Rabi model can be analyzed in terms of the actual resources involved, that is, the interrogation time t and the mean occupation of the cavity mode $\langle \hat{n} \rangle_{\text{st}}$. Hereby $\text{HL} \sim t^2 \langle \hat{n} \rangle_{\text{st}}^2 \sim t^2 \eta$. From Eqs. (20) and (21), we have $I_\omega(t, \eta) \sim (\kappa t/\eta) \times \text{HL}$ in the transient regime $\kappa t \lesssim \eta$, whereas $I_\omega(t, \eta) \sim (\eta/\kappa t) \times \text{HL}$ in the long-time regime $\kappa t \gg \eta$. Therefore, the global QFI manifests super-Heisenberg scaling with respect to the interrogation time t (the cavity photon number $\langle \hat{n} \rangle_{\text{st}}$) in the transient (long-time) regime, nevertheless is always upper bounded by the HL. We further note that $I_\omega(t_*, \eta) \sim \text{HL}$ at $t_* = \eta/\kappa$, i.e., the global QFI saturates the HL in the asymptotic limit $t, \eta \rightarrow \infty$ with $\kappa t \simeq \eta$ kept fixed. These features are illustrated in Fig. 1(b).

C. Photon counting and the scaling laws of the Fisher Information

Let us now analyze a continuous-measurement-based sensing protocol for accessing the criticality-enhanced precision scaling with open quantum sensors. As a concrete illustration, we consider the sensing of the cavity mode frequency ω of the open Rabi model via photon counting. Generalization to other types of continuous measurement, e.g., homodyning [31], is straightforward.

We assume the photons leaked from the cavity are directed to and counted by a photon detector [cf. Fig. 1(a)]. For simplicity, we assume unit detection efficiency (finite detection efficiency reduces the FI by an overall factor nevertheless does not change its scaling, see [60]). The evolution of the joint cavity-qubit system is therefore subjected to the measurement back-action conditioned on a specific series of photon detection events. Specifically, in an infinitesimal time interval $d\tau$, the detection

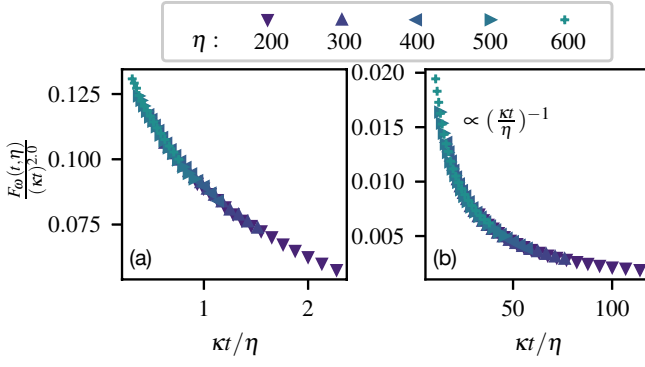


FIG. 4. Finite-size scaling of the FI $F_\omega(t, \eta)$ [cf., Eq. (24)], for the photon counting signals of the critical open Rabi model ($g = g_c$), in both (a) the transient regime $\kappa t \lesssim \eta$ and (b) the long-time regime $\kappa t \gg \eta$. Each data point represents an average of 10^5 independent trajectories in (a), whereas 10^4 independent trajectories in (b). The sampling numbers are chosen such that the error associated with finite sampling is sufficiently small, cf. Fig. 5.

of a photon leads to the collapse of the (unnormalized) conditional state of the cavity-qubit system according to $|\tilde{\psi}_c\rangle \rightarrow \sqrt{\kappa dt} \hat{c} |\tilde{\psi}_c\rangle$, while if no photon is detected, the system evolves according to the non-unitary dynamics $|\tilde{\psi}_c\rangle \rightarrow \hat{M}_0 |\tilde{\psi}_c\rangle$ with $\hat{M}_0 = \hat{1} - d\tau(i\hat{H} + \kappa\hat{c}^\dagger\hat{c}/2)$ [51–53, 61]. For an infinitesimal time interval $d\tau$, the probability of the detection of a photon is $p_1 = \kappa \langle \hat{c}^\dagger \hat{c} \rangle_c d\tau$ with $\langle \dots \rangle_c := \langle \tilde{\psi}_c | \dots | \tilde{\psi}_c \rangle / \langle \tilde{\psi}_c | \tilde{\psi}_c \rangle$, whereas the probability of the detection of no photon is $p_0 = \langle \hat{M}_0^\dagger \hat{M}_0 \rangle_c = 1 - p_1$. Repeating such *stochastic* evolution for each time step $[\tau, \tau + d\tau]$, in which $\tau \in [0, t]$, defines a quantum trajectory consisting of the photon detection signals up to time t and the associated conditional quantum state $|\psi_c(t)\rangle$.

Mathematically, this can be formulated rigorously in terms of a (Itô) stochastic Schrödinger equation [51–53]

$$d|\tilde{\psi}_c\rangle = -\left(i\hat{H} + \frac{\kappa}{2}\hat{c}^\dagger\hat{c}\right)dt|\tilde{\psi}_c\rangle + dN(t)(\sqrt{\kappa dt}\hat{c} - \hat{1})|\tilde{\psi}_c\rangle. \quad (22)$$

Here $dN(t)$ is a stochastic Poisson increment that takes two values: $dN(t) = 0$ with probability p_0 , and $dN(t) = 1$ with probability p_1 . The last term of Eq. (22) accounts for the back-action of photon counting by updating the system state conditioned on the detection of a photon or not. Corresponding to Eq. (22), the photon counting signal up to time t for a specific trajectory is $D(t, 0) := \{dN(ndt), \dots, dN(dt), dN(0)\}$ where we identify $t \equiv ndt$. The probability of this trajectory is [51–53]

$$P[D(t, 0)] = p_{dN(ndt)} \cdots p_{dN(0)} = \langle \tilde{\psi}_c(t) | \tilde{\psi}_c(t) \rangle. \quad (23)$$

An ensemble average over all conditional states leads to the definition of a density operator of the cavity-qubit system, $\rho(t) = \sum_{D(t, 0)} |\psi_c(t)\rangle \langle \tilde{\psi}_c(t)|$, which evolves according to the LME (19).

A single interrogation of our sensing protocol, therefore, corresponds to a quantum trajectory consisting of

the continuously detected signal $D(t, 0)$ and the associated conditional evolution of the open system. Processing $D(t, 0)$ via standard means (e.g., via Bayesian inference [29–31]) provides an estimator ω_{est} of the cavity mode frequency. The associated precision is quantified by the Fisher information (FI) of the detected signal

$$F_\omega(t) = \sum_{D(t, 0)} P[D(t, 0)] \{\partial_\omega \ln P[D(t, 0)]\}^2. \quad (24)$$

The FI (24) can be extracted numerically, via approximating the ensemble average $\sum_{D(t, 0)}$ by a statistical average over sufficient (but finite) numbers of sampled trajectories. For each trajectory, we extract $P[D(t, 0)]$ via Eq. (23) following the numerical propagation of Eq. (22), and $\partial_\omega P[D(t, 0)]$ via calculating $P[D(t, 0)]$ at a slightly different ω and subsequent numerical differentiation.

In Fig. 4 we show the results of our numerical finite-size scaling of the FI for different system sizes η in both the transient regime $\kappa t \lesssim \eta^z$ [Fig. 4(a)] and in the long-time regime $\kappa t \gg \eta^z$ [Fig. 4(b)], assuming the model is tuned at the CP $g = g_c$. The perfect data collapse indicates, similar to the global QFI, that the FI obeys scaling behavior at criticality,

$$F_\omega(t, \eta) = (\kappa t)^2 f_F(\kappa t / \eta), \quad \kappa t \lesssim \eta, \quad (25)$$

$$F_\omega(t, \eta) = \text{const.} \times \kappa t \eta, \quad \kappa t \gg \eta. \quad (26)$$

where $f_F(\kappa t / \eta)$ is a universal function reflecting the finite-size correction.

As a validation of the accuracy of our numerics, we show in Fig. 5 the convergence of the approximated FI with respect to N_{traj} , the number of sampled trajectories. As can be seen, the approximated FI gradually converges to the predicted scaling form (cf. Fig. 4) as N_{traj} increases, while convincing data collapse typically requires $N_{\text{traj}} \geq 10^4$. As the simulation time of each trajectory scales polynomially in the system size at criticality, the extraction of such FI scaling for generic dissipative criticality in high spatial dimensions may represent a computational challenge. Here, thanks to its zero-dimensional, finite-component nature, our model system allows for extracting such scaling behavior directly by quantum trajectory simulation.

D. Discussion

In contrast to the global QFI, we are not able to relate analytically the scaling laws of the FI (25) and (26) to the critical exponents of the underlying CP. Nevertheless, we manage to develop a physical understanding of these scaling laws by analyzing them with respect to the resources involved in our sensing protocol. First, the long-time behavior Eq. (26) can be expressed as $F_\omega(t, \eta) \sim \kappa^2 t t_*$ with $t_* \simeq \eta / \kappa$ as defined previously in Sec. III B. This should be compared to the long-time behavior of the global QFI (21), which can be expressed similarly as

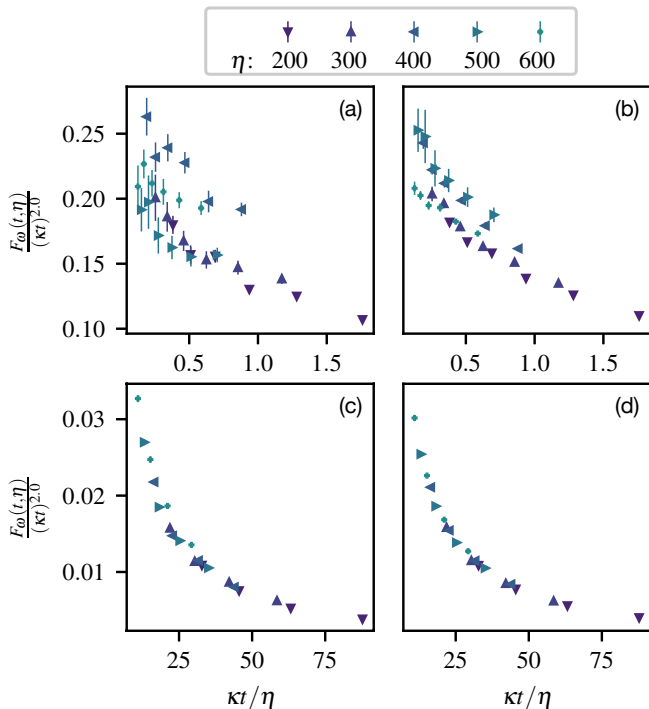


FIG. 5. Convergence of the FI (24) with respect to the number of sampled trajectories N_{traj} . In (a) and (c) $N_{\text{traj}} = 10^3$, while in (b) and (d) $N_{\text{traj}} = 10^4$. The error bars are estimated from the variance of 10 independent samplings, and are not shown if they are smaller than the data point size. The FI converges more slowly in the transient regime [(a) and (b)] than in the long-time regime [(c) and (d)], as represented by larger error bars in the former. By sampling a sufficient number of trajectories we reduce the sampling error in the FI, leading to the caling collapse as shown in Fig. 4.

$I_\omega(t, \eta) \sim \kappa^2 t t_* \langle \hat{n} \rangle_{\text{st}}^2$ (note that $\langle \hat{n} \rangle_{\text{st}} \sim \eta^{1/2}$ at the CP, as introduced in Sec. III A). Such an expression illustrates that the global QFI (21) behaves the same as that of a standard noiseless interferometric scheme involving $\langle \hat{n} \rangle_{\text{st}}$ entangled photons and spanning a time window t_* in each interrogation. The time scale t_* therefore characterizes the correlation time of the emitted photons—two photon detection events that are separated by more than t_* are essentially uncorrelated and therefore are analogous to two independent interrogations. Such an interpretation extends naturally to the FI—in comparison to the global QFI, it lacks the contribution $\sim \langle \hat{n} \rangle_{\text{st}}^2$ from the cavity photons, as it is obtained by measurement of the environment alone.

In contrast to these long-time scalings, the transient scaling Eq. (25) is due to dynamic critical behavior that lacks an analog in conventional interferometric schemes. Nevertheless, it can be recovered from the long-time scaling Eq. (26) by the simple replacement $\eta \rightarrow (\kappa t)^{1/z}$, as they both originate from the dynamic criticality of the underlying CP, with $\eta^{-1} [(\kappa t)^{-1/z}]$ being the dominant perturbation in the long-time (transient) regime respectively. Similarly for the global QFI, Eq. (20) can be re-

lated to (21) by the same replacement.

Finally, we compare the precision bounds of our continuous-measurement-based sensing protocol with that based on direct measurement of the critical steady state of the open Rabi model [23]. The latter scheme discards the emitted radiation quanta and, therefore, the achievable sensing precision of it is upper-bounded by the QFI of the reduced density matrix of the cavity-qubit system. Such a QFI was shown [23] to obey the SQL, i.e., $\sim \kappa t \langle \hat{n} \rangle_{\text{st}} \sim \kappa t \eta^{1/2}$, where the linear dependence on t results from repeated preparation of the steady state in every interrogation. By continuously counting the emitted radiation quanta, the precision scaling is enhanced as quantified by the FI in the long-time regime $F_\omega(t, \eta) \sim \kappa t \eta$. Moreover, in our scheme the global QFI in the long-time regime obeys a further enhanced scaling $I_\omega(t, \eta) \sim \kappa t \eta^2$, which can in principle be achieved by a joint measurement of the open system and the environment.

IV. CONCLUSION AND OUTLOOK

In contrast to the previous state-of-the-art, we have established a protocol for criticality enhanced sensing via continuous observation of the radiation quanta emitted by critical open sensors. The resulting precision achieves significantly enhanced scaling, thereby establishing the metrological usefulness of the emitted radiation quanta. To achieve this, we have followed a two-fold approach.

First, we establish a scaling theory for the global QFI at a continuous dissipative CP. Under general assumptions, we demonstrate that the global QFI obeys transient and long-time scaling laws governed by the universal critical exponents of the underlying CP. Such scaling can be super-Heisenberg with respect to the interrogation time t or the particle number N , but not both. We show that the global QFI is close to and can in principle saturate the HL at dissipative criticality, therefore providing rich opportunities towards criticality enhanced quantum sensing. To achieve such a precision limit, however, requires the most general measurement of the joint system-environment, which may be challenging in practice.

In view of this, we present a feasible sensing scheme for approaching such criticality-enhanced precision scaling, based on continuous measurement of the radiation quanta emitted by the open sensor. We illustrate our protocol via counting photons emitted by a critical open sensor—the open Rabi model. The relatively simple structure of this model allows us to extract the FI of the detected signal, as a key parameter quantifying the achievable precision of our protocol. Similar to the global QFI, the FI manifests (transient and long-time) scaling behavior at the CP which, importantly, exceeds the SQL and therefore is criticality-enhanced. Moreover, as the QFI of the reduced density matrix of the open Rabi model obeys the SQL [23], our protocol outperforms any

protocol based on direct measurement of the open sensor alone. Such a continuous measurement based sensing scheme can be applied to various open quantum sensors permitting continuous readout, thereby establishing a general and practical strategy for criticality enhanced sensing with open quantum sensors.

The quantum sensing framework established in the present work is timely and feasible in view of the significant experimental progresses in recent years towards the integration of synthetic many-body systems as quantum sensors. Promising candidates for directly implementing our model system include the recent realization of the critical Rabi Hamiltonian in trapped-ion setups [62], where continuous readout is a well-established tool. Several experimental platforms have demonstrated the intimately related open Dicke model [63, 64], which lies in the same universality class as the open Rabi model and therefore shares the same criticality enhanced precision. Other relevant systems where our general theory may apply include optically addressable spins in solid, e.g., color centers in diamond [65], two-dimensional surfaces on diamond [66], driven-dissipative atomic gas [67, 68], polariton condensates [69] and many-body cavity QED [70] and circuit QED [71] setups. With its broad applicability, our sensing protocol may lead to significant improvements to the design of ultimate sensing devices on the basis of interacting many body systems that may, for example, find applications in human-machine interfaces [72] or heart diagnostics [73].

The present work raises a few interesting theoretical questions as well. For example, while the general scaling theory of the global QFI (cf. Sec. II) established here are validated numerically for the open Rabi(Dicke) universality class, we believe they and the underlying scaling assumptions hold for a broad class of dissipative CPs, including CPs in higher spatial dimensions. Extending such analysis to models belonging to other universality classes and evaluating the associated metrological precision limit therefore represents an attractive theoretical problem. In the broad context of open quantum sensors, remaining open questions include how to achieve the criticality-enhanced scaling of the global QFI via realistic measurement schemes, and the possible generalization of present results to non-Markovian scenarios [74]. Finally, as the QFI is a witness of multipartite entanglement [75, 76], the universal scaling of the global QFI at dissipative criticality may lead to interesting implications, e.g., to the study of the dynamics of entanglement and other correlations in critical open quantum systems.

ACKNOWLEDGMENTS

This work was supported by the ERC Synergy grant HyperQ (Grant No. 856432), the EU projects HYPERDIAMOND (Grant No. 667192) and AsteriQs (Grant No. 820394), the QuantERA project NanoSpin (13N14811) and the BMBF project DiaPol (13GW

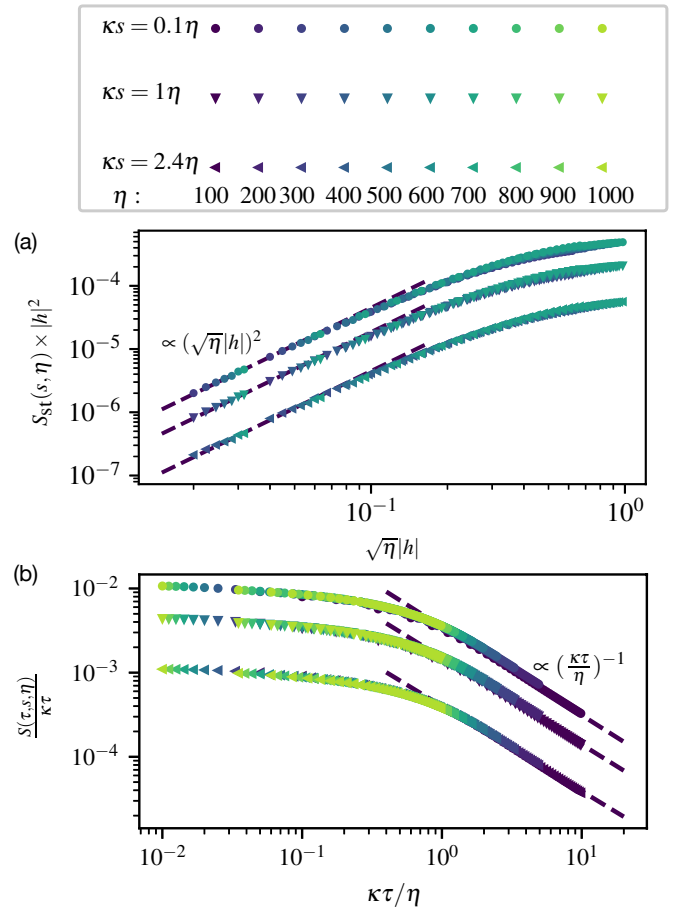


FIG. 6. Numerical verification of the dynamic scaling ansatz (10) for the open Rabi model, which has $z = 1$, $\nu = 2$ and $\Delta_{\hat{n}} = -1/2$. The perfect scaling collapse demonstrates the validity of Eq. (10) along specific axis in the parameter space (see text).

0281C). We acknowledge support by the state of Baden-Württemberg through bwHPC and the German Research Foundation (DFG) through grant no INST 40/575-1 FUGG (JUSTUS 2 cluster). Part of the numerical simulations were performed using the QuTiP library [77].

Appendix A: Numerical validation of the dynamic scaling ansatz

Here we provide a validation of the dynamic scaling ansatz (10) for the open Rabi model. Equation (10) prescribes that the correlator $S(\tau, s, L)$ obeys a universal scaling form determined by three relevant perturbations h , τ^{-1} and L^{-1} , which can be validated via finite-size scaling collapse in the $(h, \tau^{-1}, L^{-1}, s^{-1})$ parameter space. For illustration, in the following we fix either τ^{-1} or L^{-1} , and show numerical finite-size scaling of the correlator with respect to the other two perturbations. To be specific, we choose $\hat{O} = \hat{n}$ which has scaling dimension $\Delta_{\hat{n}} = -1/2$ (cf. Sec. III A).

First, we fix $\tau^{-1} = 0$, which corresponds to taking the infinitely long time limit, at which $S(\tau, s, \eta) = S_{\text{st}}(s, \eta)$. In Fig. 6 (a), we show the results of our numerical finite-size scaling of $S_{\text{st}}(s, \eta)$ for different η and $h = g - g_c$ at various κs (which serves as an irrelevant perturbation). The perfect scaling collapse indicates, at sufficiently large $|h|$, $|h| \gg \eta^{-1/\nu}$, h is the dominant perturbation and correspondingly $S_{\text{st}}(s, \eta) \sim |h|^{2\nu\Delta_{\hat{n}}} = h^{-2}$. In contrast, at small h the inverse system size η^{-1} is the dominant perturbation, and correspondingly $S_{\text{st}}(s, \eta) \sim \eta^{-2\Delta_{\hat{n}}} = \eta$. These demonstrate the validity of Eq. (10) along the axis $\tau^{-1} = 0$.

Next, we fix $h = 0$, and perform finite-size scaling of $S(\tau, s, \eta)$ for different η and τ at various κs , as shown in Fig. 6 (b). The perfect scaling collapse indicates, at sufficiently small τ^{-1} , the inverse system size η^{-1} is the dominant perturbation and correspondingly $S(\tau, s, \eta) \sim \eta^{-2\Delta_{\hat{n}}} = \eta$, whereas at large τ^{-1} the scaling form becomes $S_{\text{st}}(s, \eta) \sim \tau^{-2\Delta_{\hat{n}}/z} = \tau$. These demonstrate the validity of Eq. (10) along the axis $h = 0$.

Similar procedure can be carried out for all the parameter space $(h, \tau^{-1}, L^{-1}, s^{-1})$ surrounding the CP, which validates Eq. (10).

Appendix B: Numerical calculation of the global quantum Fisher information

We follow an efficient method proposed in Ref. [42] to numerically calculate the global QFI of the joint system-environment, which we summarize here to keep our work self-contained. The starting point is an alternative expression of the QFI equivalent to Eq. (1) of the main text,

$$I_{\theta}(t) = 4\partial_{\theta_1}\partial_{\theta_2}(\log |\langle \Psi_{\theta_1}(t) | \Psi_{\theta_2}(t) \rangle|)|_{\theta_1=\theta_2=\theta}, \quad (\text{B1})$$

where $|\Psi_{\theta_1}(t)\rangle$ is the pure global state of the system plus the environment at time t . Although a complete knowledge of the global quantum state is impractical as the number of photons in the environment increases with time, in [42] the authors describe an efficient way to calculate the QFI without accessing the full quantum state. The main idea is that as long as the Born-Markov approximation is valid we can discretize time such that in every time interval $[t_i, t_i + \delta t)$ the system interacts with independent environmental degrees of freedom. As a result, at time $t = N\delta t$, the state of the joint system-bath $|\Psi(t)\rangle$ can be expressed as an entangled state in the tensor-product Hilbert space of the open system and N environmental subspaces

$$|\Psi(t)\rangle = \hat{U}_{t_{N-1}}\hat{U}_{t_{N-2}}\cdots\hat{U}_{t_0}|\psi(0)\rangle|0_{N-1},\cdots 0_0\rangle, \quad (\text{B2})$$

where $|\psi(0)\rangle$ is the initial state of the system, \hat{U}_{t_i} are the unitary operators acting on the open system and the environment Hilbert space associated to time t_i . Here we have also associated an L -dimensional Hilbert space for each environment subspace $\{|m_i\rangle\}, m = 0, 1, \dots, L-1$, and assumed that each of them are initialized in the vacuum $|0_i\rangle$ before the interaction. In turn, we can introduce ‘measurement effect operators’, \hat{M}_{m_i} which define the evolution of the open quantum system with the associated transfer of the environment from state $|0_i\rangle$ to $|m_i\rangle$ and write

$$|\Psi(t)\rangle = \sum_{m_0\cdots m_{N-1}=0}^{M-1} \hat{M}_{m_{L-1}}\cdots\hat{M}_{m_0}|\psi(0)\rangle \otimes |m_{N-1},\cdots m_0\rangle \quad (\text{B3})$$

A particular choice of $m_0\cdots m_{N-1}$ which corresponds to a single term in Eq. (B3) defines the quantum stochastic trajectory $|\psi_c(t)\rangle \propto \hat{M}_{m_{N-1}}\cdots\hat{M}_{m_0}|\psi(0)\rangle$. The unknown parameter, θ , that we want to estimate is encoded in the unitary operators U_{t_i} and hence the measurement effect operators M_{m_i} . After tracing out the environment degrees of freedom we obtain the reduced density matrix that describes the open quantum system and evolves according to the equation:

$$\frac{d\rho(t)}{dt} = \left(\sum_{m=0}^{L-1} \hat{M}_m \rho(t) \hat{M}_m^\dagger - \rho(t) \right) / \delta t \quad (\text{B4})$$

For infinitesimal time step δt this gives rise to the standard Lindblad master equation as described in the main text. Going back to Eq.(B1) notice that the inner product $\langle \Psi_{\theta_1} | \Psi_{\theta_2} \rangle$ can be written as $\text{Tr}_{\text{sys,env}}\{|\Psi_{\theta_1}\rangle\langle\Psi_{\theta_2}|\} = \text{Tr}_{\text{sys}}\{\rho_{\theta_1,\theta_2}\}$ where the action of the operators $M_{m_{N-1}}(\theta_1)\cdots M_{m_0}(\theta_1)$ from the left and $M_{m_0}^\dagger(\theta_2)\cdots M_{m_{N-1}}^\dagger(\theta_2)$ from the right, has been absorbed in the definition of ρ_{θ_1,θ_2} . This is similar to Eq. (B4) and thus ρ_{θ_1,θ_2} is the solution of a generalized master equation (ME) $d\rho/dt = \mathcal{L}_{\theta_1,\theta_2}\rho$. Specifically to our case that the unknown parameter is encoded in the Hamiltonian of the open system, the generalized ME can be derived to be

$$\mathcal{L}_{\theta_1,\theta_2}\rho = -i\hat{H}(\theta_1)\rho + i\rho\hat{H}(\theta_2) + \sum_{\ell} \left(\hat{J}_{\ell}\rho\hat{J}_{\ell}^\dagger - \frac{1}{2}\{\hat{J}_{\ell}^\dagger\hat{J}_{\ell},\rho\} \right).$$

We can solve the generalized ME numerically for (θ_1, θ_2) in the neighborhood of (θ, θ) and determine the global QFI by numerical difference via Eq. (B1).

[1] V. B. Braginskii and Y. I. Vorontsov, *Soviet Physics Uspekhi* **17**, 644 (1975).

[2] C. M. Caves, *Phys. Rev. Lett.* **45**, 75 (1980).

[3] C. M. Caves, K. S. Thorne, R. W. P. Drever, V. D. Sand-

- berg, and M. Zimmermann, *Rev. Mod. Phys.* **52**, 341 (1980).
- [4] C. M. Caves, *Phys. Rev. D* **23**, 1693 (1981).
 - [5] V. Giovannetti, S. Lloyd, and L. Maccone, *Science* **306**, 1330 (2004).
 - [6] D. J. Wineland, J. J. Bollinger, W. M. Itano, F. L. Moore, and D. J. Heinzen, *Phys. Rev. A* **46**, R6797 (1992).
 - [7] D. M. Greenberger, M. A. Horne, and A. Zeilinger, *Bell's Theorem, Quantum Theory, and Conceptions of the Universe*, edited by M. Kafatos, 69-72 (Kluwer, Dordrecht., 1989).
 - [8] M. Kitagawa and M. Ueda, *Phys. Rev. A* **47**, 5138 (1993).
 - [9] S. F. Huelga, C. Macchiavello, T. Pellizzari, A. K. Ekert, M. B. Plenio, and J. I. Cirac, *Phys. Rev. Lett.* **79**, 3865 (1997).
 - [10] H. Strobel, W. Muessel, D. Linnemann, T. Zibold, D. B. Hume, L. Pezzè, A. Smerzi, and M. K. Oberthaler, *Science* **345**, 424 (2014).
 - [11] J. G. Bohnet, B. C. Sawyer, J. W. Britton, M. L. Wall, A. M. Rey, M. Foss-Feig, and J. J. Bollinger, *Science* **352**, 1297 (2016).
 - [12] X.-Y. Luo, Y.-Q. Zou, L.-N. Wu, Q. Liu, M.-F. Han, M. K. Tey, and L. You, *Science* **355**, 620 (2017).
 - [13] A. Omran, H. Levine, A. Keesling, G. Semeghini, T. T. Wang, S. Ebadi, H. Bernien, A. S. Zibrov, H. Pichler, S. Choi, J. Cui, M. Rossignolo, P. Rembold, S. Montangero, T. Calarco, M. Endres, M. Greiner, V. Vuletić, and M. D. Lukin, *Science* **365**, 570 (2019).
 - [14] C. Song, K. Xu, H. Li, Y.-R. Zhang, X. Zhang, W. Liu, Q. Guo, Z. Wang, W. Ren, J. Hao, H. Feng, H. Fan, D. Zheng, D.-W. Wang, H. Wang, and S.-Y. Zhu, *Science* **365**, 574 (2019).
 - [15] R. Kaubruegger, D. V. Vasilyev, M. Schulte, K. Hammerer, and P. Zoller, “Quantum variational optimization of ramsey interferometry and atomic clocks,” (2021), [arXiv:2102.05593 \[quant-ph\]](https://arxiv.org/abs/2102.05593).
 - [16] C. D. Marciniak, T. Feldker, I. Pogorelov, R. Kaubruegger, D. V. Vasilyev, R. van Bijnen, P. Schindler, P. Zoller, R. Blatt, and T. Monz, “Optimal metrology with variational quantum circuits on trapped ions,” (2021), [arXiv:2107.01860 \[quant-ph\]](https://arxiv.org/abs/2107.01860).
 - [17] D. Braun, G. Adesso, F. Benatti, R. Floreanini, U. Marzolino, M. W. Mitchell, and S. Pirandola, *Rev. Mod. Phys.* **90**, 035006 (2018).
 - [18] P. Zanardi, M. G. A. Paris, and L. Campos Venuti, *Phys. Rev. A* **78**, 042105 (2008).
 - [19] M. Tsang, *Phys. Rev. A* **88**, 021801 (2013).
 - [20] M. M. Rams, P. Sierant, O. Dutta, P. Horodecki, and J. Zakrzewski, *Phys. Rev. X* **8**, 021022 (2018).
 - [21] S. Fernández-Lorenzo and D. Porras, *Phys. Rev. A* **96**, 013817 (2017).
 - [22] T. L. Heugel, M. Biondi, O. Zilberberg, and R. Chitra, *Phys. Rev. Lett.* **123**, 173601 (2019).
 - [23] L. Garbe, M. Bina, A. Keller, M. G. A. Paris, and S. Felicetti, *Phys. Rev. Lett.* **124**, 120504 (2020).
 - [24] Y. Chu, S. Zhang, B. Yu, and J. Cai, *Phys. Rev. Lett.* **126**, 010502 (2021).
 - [25] I. Bloch, J. Dalibard, and W. Zwerger, *Rev. Mod. Phys.* **80**, 885 (2008).
 - [26] R. Blatt and C. F. Roos, *Nature Physics* **8**, 277 (2012).
 - [27] A. A. Houck, H. E. Türeci, and J. Koch, *Nature Physics* **8**, 292 (2012).
 - [28] A. Keesling, A. Omran, H. Levine, H. Bernien, H. Pichler, S. Choi, R. Samajdar, S. Schwartz, P. Silvi, S. Sachdev, P. Zoller, M. Endres, M. Greiner, V. Vuletić, and M. D. Lukin, *Nature* **568**, 207 (2019).
 - [29] S. Gammelmark and K. Mølmer, *Phys. Rev. A* **87**, 032115 (2013).
 - [30] A. H. Kiilerich and K. Mølmer, *Phys. Rev. A* **89**, 052110 (2014).
 - [31] A. H. Kiilerich and K. Mølmer, *Phys. Rev. A* **94**, 032103 (2016).
 - [32] K. Baumann, C. Guerlin, F. Brennecke, and T. Esslinger, *Nature* **464**, 1301 (2010).
 - [33] J. Klinder, H. Keßler, M. Wolke, L. Mathey, and A. Hemmerich, *Proceedings of the National Academy of Sciences* **112**, 3290 (2015).
 - [34] M. P. Baden, K. J. Arnold, A. L. Grimsmo, S. Parkins, and M. D. Barrett, *Phys. Rev. Lett.* **113**, 020408 (2014).
 - [35] S. R. K. Rodriguez, W. Casteels, F. Storme, N. Carlon Zambon, I. Sagnes, L. Le Gratiet, E. Galopin, A. Lemaître, A. Amo, C. Ciuti, and J. Bloch, *Phys. Rev. Lett.* **118**, 247402 (2017).
 - [36] M. Fitzpatrick, N. M. Sundaresan, A. C. Y. Li, J. Koch, and A. A. Houck, *Phys. Rev. X* **7**, 011016 (2017).
 - [37] J. M. Fink, A. Dombi, A. Vukics, A. Wallraff, and P. Domokos, *Phys. Rev. X* **7**, 011012 (2017).
 - [38] T. P. Purdy, R. W. Peterson, and C. A. Regal, *Science* **339**, 801 (2013).
 - [39] C. J. Hood, T. W. Lynn, A. C. Doherty, A. S. Parkins, and H. J. Kimble, *Science* **287**, 1447 (2000).
 - [40] P. Bushev, D. Rotter, A. Wilson, F. Dubin, C. Becher, J. Eschner, R. Blatt, V. Steixner, P. Rabl, and P. Zoller, *Phys. Rev. Lett.* **96**, 043003 (2006).
 - [41] Z. K. Mineev, S. O. Mundhada, S. Shankar, P. Reinhold, R. Gutiérrez-Jáuregui, R. J. Schoelkopf, M. Mirrahimi, H. J. Carmichael, and M. H. Devoret, *Nature* **570**, 200 (2019).
 - [42] S. Gammelmark and K. Mølmer, *Phys. Rev. Lett.* **112**, 170401 (2014).
 - [43] S. Schmitt, T. Gefen, F. M. Stürner, T. Unden, G. Wolff, C. Müller, J. Scheuer, B. Naydenov, M. Markham, S. Pezzagna, J. Meijer, I. Schwarz, M. Plenio, A. Retzker, L. P. McGuinness, and F. Jelezko, *Science* **356**, 832 (2017).
 - [44] B. Tratzmiller, Q. Chen, I. Schwartz, S. F. Huelga, and M. B. Plenio, *Phys. Rev. A* **101**, 032347 (2020).
 - [45] K. Macieszczak, M. Guta, I. Lesanovsky, and J. P. Garrahan, *Phys. Rev. A* **93**, 022103 (2016).
 - [46] F. Albarelli, M. A. C. Rossi, D. Tamascelli, and M. G. Genoni, *Quantum* **2**, 110 (2018).
 - [47] M. B. Plenio and S. F. Huelga, *Phys. Rev. A* **93**, 032123 (2016).
 - [48] M.-J. Hwang, P. Rabl, and M. B. Plenio, *Phys. Rev. A* **97**, 013825 (2018).
 - [49] S. M. Kay, *Fundamentals of Statistical Signal Processing: Estimation Theory* (Prentice Hall, 1997).
 - [50] A. Rivas and S. F. Huelga, *Open Quantum Systems* (Springer Berlin Heidelberg, 2012).
 - [51] H. Carmichael, *An Open Systems Approach to Quantum Optics* (Springer, Berlin, 1993).
 - [52] C. Gardiner and P. Zoller, *Quantum Noise* (Springer, 2004).
 - [53] H. M. Wiseman and G. J. Milburn, *Quantum Measurement and Control* (Cambridge University Press, 2009).
 - [54] J. Cardy, *Scaling and Renormalization in Statistical Physics* (Cambridge University Press, 1996).
 - [55] D. Rossini and E. Vicari, *Phys. Rev. Research* **2**, 023211

- (2020).
- [56] A. Pelissetto, D. Rossini, and E. Vicari, *Phys. Rev. E* **97**, 052148 (2018).
 - [57] M.-J. Hwang, R. Puebla, and M. B. Plenio, *Phys. Rev. Lett.* **115**, 180404 (2015).
 - [58] F. Dimer, B. Estienne, A. S. Parkins, and H. J. Carmichael, *Phys. Rev. A* **75**, 013804 (2007).
 - [59] D. Nagy, G. Kónya, G. Szirmai, and P. Domokos, *Phys. Rev. Lett.* **104**, 130401 (2010).
 - [60] T. Ilias *et al.*, in preparation.
 - [61] M. B. Plenio and P. L. Knight, *Rev. Mod. Phys.* **70**, 101 (1998).
 - [62] M. L. Cai, Z. D. Liu, W. D. Zhao, Y. K. Wu, Q. X. Mei, Y. Jiang, L. He, X. Zhang, Z. C. Zhou, and L. M. Duan, *Nature Communications* **12**, 1126 (2021).
 - [63] K. Baumann, C. Guerlin, F. Brennecke, and T. Esslinger, *Nature* **464**, 1301 (2010).
 - [64] Z. Zhiqiang, C. H. Lee, R. Kumar, K. J. Arnold, S. J. Masson, A. S. Parkins, and M. D. Barrett, *Optica* **4**, 424 (2017).
 - [65] M. Raghunandan, J. Wrachtrup, and H. Weimer, *Phys. Rev. Lett.* **120**, 150501 (2018).
 - [66] J. Cai, A. Retzker, F. Jelezko, and M. B. Plenio, *Nature Physics* **9**, 168 (2013).
 - [67] S. Diehl, E. Rico, M. A. Baranov, and P. Zoller, *Nature Physics* **7**, 971 (2011).
 - [68] T. E. Lee, H. Häffner, and M. C. Cross, *Phys. Rev. A* **84**, 031402 (2011).
 - [69] T. Boulier, M. J. Jacquet, A. Maître, G. Lerario, F. Claude, S. Pigeon, Q. Glorieux, A. Bramati, E. Giacobino, A. Amo, and J. Bloch, “Microcavity polaritons for quantum simulation,” (2020), [arXiv:2005.12569 \[cond-mat.quant-gas\]](https://arxiv.org/abs/2005.12569).
 - [70] H. Ritsch, P. Domokos, F. Brennecke, and T. Esslinger, *Rev. Mod. Phys.* **85**, 553 (2013).
 - [71] R. Ma, B. Saxberg, C. Owens, N. Leung, Y. Lu, J. Simon, and D. I. Schuster, *Nature* **566**, 51 (2019).
 - [72] R. Zhang, W. Xiao, Y. Ding, Y. Feng, X. Peng, L. Shen, C. Sun, T. Wu, Y. Wu, Y. Yang, Z. Zheng, X. Zhang, J. Chen, and H. Guo, *Science Advances* **6** (2020).
 - [73] K. Jensen, M. A. Skarsfeldt, H. Stærkind, J. Arnbak, M. V. Balabas, S.-P. Olesen, B. H. Bentzen, and E. S. Polzik, *Scientific Reports* **8**, 16218 (2018).
 - [74] J. Piilo, S. Maniscalco, K. Härkönen, and K.-A. Suominen, *Phys. Rev. Lett.* **100**, 180402 (2008).
 - [75] P. Hyllus, W. Laskowski, R. Krischek, C. Schwemmer, W. Wieczorek, H. Weinfurter, L. Pezzé, and A. Smerzi, *Phys. Rev. A* **85**, 022321 (2012).
 - [76] G. Tóth, *Phys. Rev. A* **85**, 022322 (2012).
 - [77] J. Johansson, P. Nation, and F. Nori, *Computer Physics Communications* **184**, 1234 (2013).